

nected with the polarization vector in the dipole approximation by the usual relations. As a result, together with the Maxwell equations, we obtain a closed system of equations for the first moments.

As in plasma theory, the first-moment approximation is valid when the characteristic times of the processes under consideration are much shorter than the relaxation times determined by the collision integrals (4.2), (4.3). For example, one of the characteristic parameters is the lifetime of the radiation (photons) in the volume occupied by the system.

With the self-consistent field the system has the particular solution

$$\langle f_{nm} \rangle = \delta_{nm} f_n, \quad P=0, \quad E=0. \quad (7.3)$$

The equations of the approximation linear in the deviations from this particular solution determine, in particular, the wave properties of the system. The values of ω and k for the waves are related by the usual dispersion equations, in which the functions ε^{\parallel} and ε^{\perp} are determined by the formulas (3.11) and (3.12). Now, however, f_n in them is the particular solution (7.3) of the equations with the self-consistent field.

The account in the present work touches upon only an extremely small fraction of the problems of the kinetic theory of electromagnetic processes in systems with strong interaction. Of these, the most interesting are problems in the kinetic theory of equilibrium and non-equilibrium coherent states, e.g., the kinetics of phase transitions in the atoms-field system, super-radiance, etc. Of course, the derivation of the corresponding kinetic equations for chemically reacting systems is of interest.

We take the opportunity to thank L. V. Keldysh for comments on the text of the manuscript.

- ¹L. D. Landau and E. M. Lifshitz, *Statisticheskaya fizika* (Statistical Physics), Nauka, M., 1976 (English translation of earlier edition published by Pergamon Press, Oxford, 1969).
- ²H. B. Callen and T. A. Welton, *Phys. Rev.* **83**, 34 (1951).
- ³R. Kubo, *J. Phys. Soc. Japan* **12**, 570 (1957).
- ⁴D. N. Zubarev, *Neravnovesnaya statisticheskaya termodinamika* (Nonequilibrium Statistical Thermodynamics), Nauka, M., 1971 (English translation published by Consultants Bureau, Plenum Press, N. Y., 1974).
- ⁵V. P. Silin and A. A. Rukhadze, *Élektromagnitnye svoistva plazmy i plazmopodobnykh sred* (Electromagnetic Properties of Plasmas and Plasma-like Media), Atomizdat, M., 1961.
- ⁶M. L. Levin and S. M. Rytov, *Teoriya ravnovesnogo teplovogo izlucheniya* (Theory of Equilibrium Thermal Radiation), Nauka, M., 1967.
- ⁷S. G. Zeiger, Yu. L. Klimontovich, P. S. Landa, E. G. Lariontsev, and E. E. Fradkin, *Volnovye i fluktuatsionnye protsessy v lazerakh* (Wave and Fluctuation Processes in Lasers), ed. Yu. L. Klimontovich, Nauka, M., 1974.
- ⁸M. Lax, *Fluktuatsii i kogerentnye yavleniya* (Fluctuations and Coherence Phenomena), Mir, M., 1974 (Russ. transl. of series of papers).
- ⁹R. Graham, *Z. Phys.* **B26**, 395 (1977).
- ¹⁰Yu. L. Klimontovich, *Kineticheskaya teoriya neideal'nogo gaza i neideal'noi plazmy* (Kinetic Theory of Nonideal Gases and Nonideal Plasmas), Nauka, M., 1975.
- ¹¹A. G. Sitenko, *Fluktuatsii i nelineinoe vzaimodeistvie voln v plazme* (Fluctuations and Nonlinear Interaction of waves in Plasmas), Nauka v Dumka, Kiev, 1977.
- ¹²Yu. A. Kukhareno, *Teor. Mat. Fiz.* **31**, 133 (1977) [*Theor. Math. Phys. (USSR)* **31** (1977)].
- ¹³J. W. Gibbs, *Elementary Principles in Statistical Mechanics*, in Vol. 2 of "The Collected Works of J. Willard Gibbs", Longmans, N. Y., 1931 (Russ. transl. Nauka, M., 1946).
- ¹⁴Yu. L. Klimontovich, *Usp. Fiz. Nauk* **101**, 577 (1970) [*Sov. Phys. Uspekhi* **13**, 480 (1971)].
- ¹⁵E. A. Asmaryan and Yu. L. Klimontovich, *Vestn. Mosk. Univ.* **3**, 273 (1974).

Translated by P. J. Shepherd

Effective pressure on the Fermi surface of zinc

A. G. Budarin, V. A. Ventsel', and A. V. Rudnev

Institute of High Pressure Physics, USSR Academy of Sciences
(Submitted 20 April 1978)
Zh. Eksp. Teor. Fiz. **75**, 1706-1713 (November 1978)

Apparatus is described for the measurements of the influence of pressure up to 140 bar on the frequencies of the oscillations in the de Haas-van Alphen effect in zinc in pulsed magnetic fields up to 100 kOe. The pressure dependence of the areas of the extremal sections of the Fermi surface serves as a confirmation of the correctness of the model proposed by Rubin and Stark (The de Haas-van Alphen Spectrum of Zinc, Preprint, University of Chicago) for all the sections observed in experiment.

PACS numbers: 71.25.Hc, 62.50. + p

The Fermi surface (FS) of zinc was investigated in detail both theoretically^{1,2} and experimentally,³⁻¹⁰ but to this day it cannot be said that its form has been finally established. In fact, on the one hand, the form of the FS agrees well with the model of almost free electrons,¹ but the presence of *d* states in the conduction

band can lead to nonlocality of the potential and consequently to a strong deviation of the FS from the form proposed in Ref. 1 in some parts of the Brillouin zone (BZ).² The interpretation of the observed oscillations in the de Haas-van Alphen effect is made difficult by the complexity of the "bare" form of the FS and by the

magnetic breakdown that is produced in zinc in the region of sufficiently weak magnetic fields. It is precisely by invoking magnetic breakdown between the cross sections of the "monster" in the second BZ through the "needle" in the third BZ and of the monster through the "pocket" in the first BZ that Rudin and Stark³ succeeded in interpreting the frequency spectrum of the oscillations in the de Haas-van Alphen effect. Inasmuch as model considerations make it possible to estimate the signs and changes of the oscillation frequencies with changing pressure, the baric coefficient $d \ln S / dp$ can serve, alongside the values of the cross sections, their angular dependences, and the angular dependences of the effective masses of the electrons, as a confirmation of any particular interpretation of the observed oscillation frequencies. To this end we have measured in the present study the baric coefficients in strong magnetic fields for all FS sections observed in the (11 $\bar{2}$ 0) plane.

EXPERIMENTAL TECHNIQUE

We used a true hydrostatic pressure transmitted by liquid helium, while the change of the oscillation frequencies were determined from the phase shift of the oscillations in a manner similar to that proposed by Templeton¹¹ in measurements in stationary magnetic fields. For metals having a complicated FS (such a metal is zinc), at any direction of the magnetic field, several extremal FS were observed simultaneously, so that a Fourier analysis is required of the recorded oscillations in order to separate the frequencies and to measure the individual phase shift of the oscillations stemming from each extremal section. In pulsed magnetic fields, using a resonance procedure to record the signal,¹² the separation of the oscillation frequencies is by electronic means and difficulties remain only in the case of strong overlap of the resonance bursts.

The phase shift of the oscillations under pressure, in the case of measurement in pulsed magnetic fields, can be measured accurate to $\sim 10\%$ at an oscilloscope sweep triggering stability $\sim 10^{-7}$ sec. It is possible, however, to use less stable triggering if one records simultaneously the oscillations from two samples, one of which is in the high-pressure vessel and the other one is not under pressure. In this case the oscillations of the second sample serve as markers relative to which the phase shift of the oscillations of the sample under pressure are measured.

A block diagram of the setup is shown in Fig. 1. The pulsed magnetic field ($H_{\max} \sim 100$ kOe) was generated in the apparatus described in Ref. 6. To synchronize the triggering of the entire system, the mechanical discharger was replaced by high-power TDZ-500 thyristors, and to turn on the apparatus at the same voltage on the capacitors (accurate to ± 1 V), the pointer-type meter was replaced by a type V2-19 digital one.

Two identical samples of the required orientation were mounted on glass holders in two identical thin-walled stainless-steel tubes of 1.35 mm diameter; one tube was connected on the upper part with the helium bath, while the other was connected to a capillary that communicated with a flask of high-purity helium. The

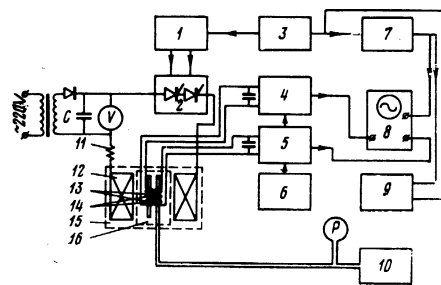


FIG. 1. Block diagram of setup: 1—Thyristor starting block, 2—dicharger, 3—G5-15 startup generator, 4—preamplifier-filter of first channel, 5—preamplifier-filter of second channel, 6—power pack for preamplifier-filters, 7—G5-26 delayed-pulse generator, 8—S1-18 oscilloscope, 9—ChZ-35 A frequency meter, 10—flask with high purity helium, 11—shunt, 12—solenoid, 13—receiving coils, 14—samples, 15—liquid nitrogen, P—manometer.

pressure was determined accurate to $\sim 1\%$ by a precision manometer. Two identical receiving coils were wound on the tubes, and formed together with parallel-connected capacitors resonant circuits tuned to $f = 33$ kHz. After amplification in preamplifier filters,⁷ the signals were applied to the two inputs of a S1-18 two-beam oscilloscope. The starting pulse was produced by a G5-15 generator and was applied to the thyristor-triggering block, to the delay generator G5-26, and to frequency meter ChZ-35A, which measured the delay time τ . The delayed pulse from the output of the generator G5-26 was fed to the oscilloscope triggering input. To observe the entire pattern of the oscillations and to perform amplitude measurements, the oscilloscope was triggered with an undelayed pulse. To measure the phase shift of the oscillations under pressure, the triggering took place at the instant of time τ corresponding to the maximum resonant burst of the oscillations of the corresponding frequency, and photographs were taken of several oscillations at a sweep $10 \mu\text{sec/cm}$ at atmospheric pressure, at several values of the pressure, and after the pressure was removed. The baric coefficient

$$\frac{d \ln S}{dp} = p^{-1} \frac{\Delta \varphi}{2\pi F} \frac{H}{F},$$

where $\Delta \varphi$ is the phase shift of the oscillations of frequency F , measured in the field H , was determined on the basis of the time τ measured with the frequency meter and of the parameters ω and δ of the damped magnetic field $H = H_0 e^{-\delta t} \sin \omega t$, using the formula

$$\frac{d \ln S}{dp} = \frac{\Delta \varphi}{2\pi F p} (\omega \operatorname{ctg} \omega \tau - \delta).$$

The error in the determination of the baric coefficient consisted in the error in the determination of $\Delta \varphi$ (15–25%), due to the width of the oscilloscope beam, and also the errors in the calibration of ω and δ ($\sim 2\%$), in the determination of τ , and in the determination of the applied pressure p . The total error ranged from 10 to 30%. The phase shift was determined reliably when the resonant burst did not overlap the neighboring bursts. In the case of a strong overlap of the bursts coming from close extremal sections, the phase shift

can differ noticeably from the phase shifts of each of the oscillations, and the sign of the shift can differ from those of the initial oscillations. This calls for the exercise of particular caution in the interpretation of the phase shifts for oscillations with beats. The measurements were therefore carried out mainly for well resolved resonance bursts.

The zinc samples required orientation were cut from a bulky single crystal and measured $10 \times 1 \times 0.8$ mm. After etching in dilute hydrochloric acid, the transverse dimensions were ~ 0.5 mm. The sample orientations was made more precise by x-ray diffraction, accurate to $\sim 1^\circ$. The axes of the investigated samples coincided with the magnetic field direction and were in the $(11\bar{2}0)$ plane.

To determine more accurately the solenoid parameter H_0 , five oscillation frequencies were chosen in the region $0 < \theta < 30^\circ$, and H_0 was determined from the known values of these frequencies.⁸ When such a calibration is used, the frequencies obtained from measurements in pulsed magnetic fields agree within 3% in the entire angle interval with the oscillation frequencies obtained in a stationary magnetic field.⁸

MEASUREMENT RESULTS

1. The FS of zinc in the model of almost free electrons¹ and in the model of the local pseudopotential is located in the first four BZ, with the first and second, as well as the third and fourth zones separated on the (0001) faces by narrow spin-orbit gaps. In the first zone are located the pockets, in the second the monster, in the third the lens, needle, and butterfly, and in the fourth the cigar. Allowance for the nonlocality of the potential² hardly influences the dimensions of all the parts of the FS, with the exception of the butterfly and the cigar, which should not exist in this approximation.

The frequency spectrum of the oscillations in zinc has a number of branches that are uniquely connected with the sections of the lens, the needle, the monster, and the pockets, and also a number of branches whose interpretation is ambiguous. The energy spectrum of the electrons in zinc has narrow gaps, so that magnetic breakdown takes place in relatively weak magnetic fields and leads to the appearance of new magnetic-breakdown sections. Rudin and Stark,⁸ starting with the absence of a butterfly or a cigar in the data of Ref. 2, proposed an interpretation of the observed oscillation frequencies by dividing them into three groups. The picture proposed by them is shown for the $(11\bar{2}0)$ plane on Fig. 2, where the solid lines were drawn in accordance with the data of Ref. 8, and the points correspond to those cases and orientations for which we measured the baric coefficients in the present paper.

According to this interpretation, the first group includes the oscillations connected with the sections of the pocket α , the monster μ , the lens λ , and the needle (not marked on Fig. 2). The second group includes the magnetic-breakdown oscillations designated by the letter A. The origin of such sections can be explained using as an example sections perpendicular to the hexa-

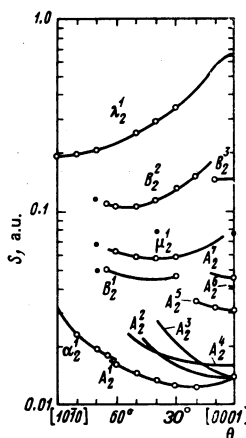


FIG. 2. Oscillation-frequency spectrum in $(11\bar{2}0)$ plane. The solid lines were drawn through the points of Ref. 8. The light circles denote frequencies for which the baric coefficient was measured. The dark points correspond to oscillations not observed in Ref. 8.

gonal axis. On the AHL plane, the pocket and monster are imbedded in each other and are separated by a spin-orbit gap. In the plane parallel to AHL but located a distance k_H from it, the arms of the monster, which are in contact along the vertical edge of the BZ, form a trefoil in which the triangle of the pocket is imbedded. With increasing k_H , the area of the section enclosed by the trefoil increases, and the area of the cross section of the pocket decreases, i.e., neither section is extremal. The magnetic breakdown can give rise to a section that encloses both the monster section and the pocket section, and turns out to be extremal. Depending on the number of breakdown acts and reflection acts, and entire set of such extremal sections is produced, and all are connected with one another by definite relations.

The third group of sections is made up of magnetic-breakdown orbits designated by the letter B. They are the result of breakdown through the needle near the point K in the BZ between the sections of the monsters located in three neighboring zones in the repeated-zone scheme. Without magnetic breakdown, the monster section $\mu_{1/2}$ is realized, and breakdown through the needle between two other sections of the monster gives rise to the section B_2^1 , while breakdown of all the gaps results in the section B_2^2 , which encloses all three parts of the monster. At $H \parallel [0001]$ there is produced, in addition, a section B_2^3 which passes on the inside of the horizontal arms of the two monsters in the repeated-zone scheme with breakdown through the needle.

Experiments performed under pressure yield additional information on the extremal sections. A comparison of the obtained baric coefficients with model representations leads to the conclusion that it is correct to identify the section with the observed oscillation frequency, and if the magnetic breakdown sections have areas connected by definite relations, the same relation should hold also between the baric coefficients.

2. The oscillations connected with the lens section were measured under pressure in the angle interval

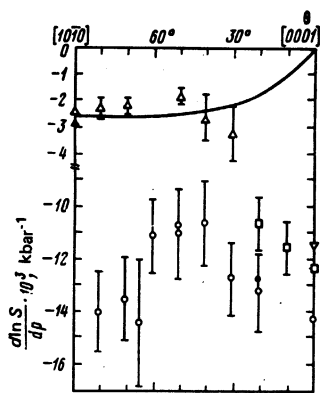


FIG. 3. Baric coefficient $(d \ln S / dp) \cdot 10^3 \text{ kbar}^{-1}$ for lens (Δ —our present data, \blacktriangle —data of Ref. 13, solid line—calculation in the 2-OPW approximation) and for the sections of group A_2^4 (\circ —for α_2^1 and A_2^1 , \square —for A_2^2 , ∇ —for A_2^3 , \bullet —data of Ref. 14 for A_2^4).

$30^\circ < \theta < 90^\circ$. The baric coefficient was negative in the entire measurement interval (Fig. 3) and agrees with the data of Ref. 13 (black triangles in Fig. 3) as well as with the calculation of $d \ln S / dp$ obtained in the 2-OPW approximation on the basis of the results of Ref. 13.

3. The frequencies of the oscillations α_2^1 and A_2^1 were observed at the angle interval $0 < \theta < 80^\circ$. In the interval $0 < \theta < 60^\circ$ the oscillation amplitude is very large, and is noticeably smaller at $60^\circ < \theta < 80^\circ$. In the region $\theta = 10^\circ$, a complicated beat picture was produced, due apparently to superposition of the frequencies of the oscillations A_2^1 , A_2^2 , A_2^3 , and A_2^4 . Under pressure, the frequencies α_2^1 and A_2^1 decrease (Fig. 3), in good agreement with the data of Ref. 14 at $\theta = 20^\circ$, while at $\theta = 50^\circ$ they agree with the value $(-10.7 \pm 1) \times 10^{-3} \text{ kbar}^{-1}$ obtained by a modulation procedure in a stationary magnetic field. Our data differ from the earlier results obtained in Ref. 13 for the frequencies of the oscillations A_2^1 , and possible causes of the discrepancy will be discussed below. Near the hexagonal axis, the results of the measurements of the influence of pressure on the frequencies of A_2^5 and A_2^7 (Fig. 3) agree with the data of Ref. 13 in the same angle interval.

At $H \parallel [0001]$ we observed small-amplitude oscillations with frequency $F = 2.9 \times 10^7 \text{ Oe}$ ($S = 0.0775 \text{ at. un.}$), which are not observed in the frequency spectrum.⁸ Under pressure this frequency decreased with a coefficient $(-10 \pm 1.5) \times 10^{-3} \text{ kbar}^{-1}$.

Thus, for the sections of this group, at magnetic-field directions close to $H \parallel [0001]$, the relations between the section areas⁸ and between the baric coefficients for these sections (the data of Ref. 13 and of the present paper) are in agreement. The negative baric coefficient indicates also that these sections belong to the monster-pocket magnetic-breakdown orbits. Oscillations with frequency $F = 2.9 \times 10^7 \text{ Oe}$ at $H \parallel [0001]$ can also be included in this group, in view of the satisfaction of the relation between the frequencies $F = F(A_2^5) + F(A_2^7)$ and the baric coefficients

$$\frac{d \ln S}{dp} = \frac{S(A_2^5)}{S} \frac{d \ln S(A_2^5)}{dp} + \frac{S(A_2^7)}{S} \frac{d \ln S(A_2^7)}{dp}.$$

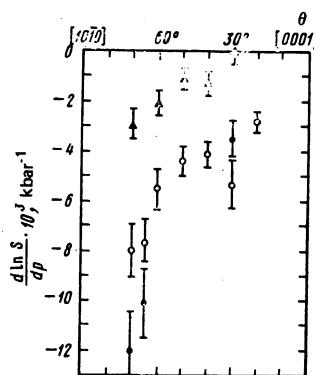


FIG. 4. Baric coefficient $(d \ln S / dp) \cdot 10^3 \text{ kbar}^{-1}$ for the sections B_2^1 (\bullet), B_2^2 (\circ), and μ_2^1 (Δ).

Indeed, $F(A_2^5) = 1.1 \times 10^7 \text{ Oe}$, $F(A_2^7) = 1.7 \times 10^7 \text{ Oe}$, $d \ln S(A_2^5) / dp = -12.3 \times 10^{-3} \text{ kbar}^{-1}$, $d \ln S(A_2^7) / dp = -11.5 \times 10^{-3} \text{ kbar}^{-1}$, $d \ln S / dp = (-10 \pm 1.5) \times 10^{-3} \text{ kbar}^{-1}$ and, accurate to 15%, $(-10 \pm 1.5) \times 10^{-3} \text{ kbar}^{-1} = -11.5 \times 10^{-3} \text{ kbar}^{-1}$.

The oscillations connected with the A_2^1 branch go over in accordance with Ref. 8 at $\theta > 60^\circ$ into oscillations connected with the section of the pocket α_2^1 (Fig. 2). The frequencies of the oscillations for the branch $A_2^1 - \alpha_2^1$ decrease under pressure (Fig. 3), and this decrease is larger at $\theta > 60^\circ$, a fact that may offer evidence in favor of dividing the branch into two groups of oscillations.

4. The oscillations corresponding to the branch B_2^2 were observed in the angle interval $20^\circ < \theta < 70^\circ$, and the oscillation frequencies decreased in the entire angle interval (Fig. 4), with a baric coefficient that ranged from $(-2.7 \pm 0.4) \times 10^{-3} \text{ kbar}^{-1}$ at 20° to $(-8 \pm 1.1) \times 10^{-3} \text{ kbar}^{-1}$ at 70° . The branch B_2^2 coincides with the branch B obtained in Ref. 5, and with that part of the branch C of the same reference (at $\theta > 55^\circ$) which was interpreted as being connected with the butterfly section. The negative baric coefficient indicates that the single $B-C$ branch coincides with the B_2^2 branch and that at $\theta > 55^\circ$ the observed oscillations cannot be identified with the butterfly section, inasmuch as the latter should have, according to all estimates, a positive baric coefficient. At $\theta = 40^\circ$ and at $T = 2.5 \text{ K}$, under evacuation, a weak burst was observed, of the same frequency as the descending part of the C branch, but whose frequency increased with pressure, with a coefficient $(+3 \pm 2) \times 10^{-3} \text{ kbar}^{-1}$. This burst, however, was close to a strong burst with frequency μ_2^1 , so that there is no absolute assurance concerning the magnitude and sign of this shift.

The oscillations of frequency μ_2^1 were investigated under pressure in the angle interval $30^\circ < \theta < 70^\circ$ (Fig. 4). At angles from 40 to 60° the oscillations had the characteristic form of beat patterns. These beats could be due either to superposition of frequencies connected with sections of the type but located in other parts of the BZ, or to superposition of the frequencies μ_2^1 and B_2^1 . To exclude, in the determination of the baric coefficient, the arrow connected with the possible

superposition of the frequencies μ_2^1 and B_2^1 , the phase shift was determined not exactly at the center of the burst, but slightly away from the center towards stronger fields. At $\theta = 65, 70,$ and 30° , the bursts from μ_2^1 and B_2^1 were distinctly separated, and the values of $d \ln S / d p$ for these angles are shown in Fig. 4. The amplitude of the oscillations with frequency B_2^1 is very small in the entire interval, and the absence of oscillations at $40^\circ < \theta < 60^\circ$ may be due to the fact that they cannot be distinguished against the background of the powerful bursts connected with the frequency μ_2^1 .

Oscillations with frequency B_2^3 were observed at $\theta = 10^\circ$ and exhibited an increase of frequency with a coefficient $(+2.2 \pm 0.6) \times 10^{-3} \text{ kbar}^{-1}$. In the 1-OPW approximation it is easy to estimate the baric coefficient for such a section; the estimate yielded the value $d \ln S(B_2^3) / d p = 3 \cdot 1 \times 10^{-3} \text{ kbar}^{-1}$, which is in good agreement with experiment and confirms the interpretation of the B_2^3 branch.

5. The main result of this paper should be taken to be the confirmation of the model proposed in Ref. 8 to explain the observed sections of the FS of zinc. No unequivocal conclusion can be drawn from our present paper concerning the existence of electron surfaces in the third and fourth BZ (butterfly-cigar). In fact, the expected positive baric coefficient could not be observed for any branch of the spectrum that might be identified with these sections. It was proposed in Ref. 5 that branches A_2^5 and A_2^7 (labelled *K* and *J* in Ref. 5) correspond to the cigar and butterfly sections, while the branch *C* (at $\theta > 50^\circ$ this section is, at any rate, close to the section B_2^2) also corresponds to the butterfly section. The negative baric coefficient for the foregoing sections rejects this interpretation. The only point at $\theta = 40^\circ$, corresponding in frequency to the descending part of the *C* branch with positive baric coefficient, can apparently not offer evidence that this point belongs to the butterfly section. It should be noted that in Ref. 5 the oscillation frequencies ascribed to the butterfly were observed with sufficient amplitudes only at $T < 2 \text{ K}$, whereas in the present paper the B_2^2 branch was reliably measured at 4.2 K and with decreasing temperature the oscillations with the frequency of the branch *C* could not be distinguished against the background of the oscillations with frequency B_2^2 .

6. We have previously measured¹³ the baric coefficients for many of the sections measured in the present paper. Our present results agree well with the data of Ref. 13 at magnetic-field orientations along the principal crystallographic directions, thus confirming the conclusion drawn in Ref. 13 that the pseudopotential depends on the pressure. At intermediate orientations, however, there is a considerable discrepancy between the present data and those of Ref. 13, and we must dwell on their causes in greater detail.

Thus, for the frequency A_2^1 we observed in Ref. 13 at $40^\circ < \theta < 70^\circ$ a positive baric coefficient. Since the earlier measurements¹³ were made in a stationary magnetic field, to exclude the possibility of an error due to the difference between the measurement procedures, we repeated the measurements under pressure in a station-

ary field at $\theta = 50^\circ$ and Fourier-analyzed the recorded oscillations. The result, $(-10.7 \pm 1) \times 10^{-3} \text{ kbar}^{-1}$, agrees well with the $(-11 \pm 1.7) \times 10^{-3} \text{ kbar}^{-1}$ obtained by measurements in pulsed magnetic fields. This gives grounds for assuming that the present results are quite reliable. The measurements in Ref. 13 were made by two methods. In the first method the samples were cut out along the principal crystallographic directions and were tightly fitted in a narrow channel of the high-pressure vessel. These results agree well with the results of the present study, so that the pseudopotential matrix element calculations made on the basis of these measurements can be regarded as perfectly reliable.

In the second method, the measurements were made in a wide range of angles with the sample rotated in a spindle placed in the high-pressure vessel. These results do not agree with our present results. The main cause of the incorrect results of Ref. 13, which were obtained by the second method, is an error in the construction of the high-pressure vessel with the spindle. In that construction, a rotating drum containing the sample was fastened on the vessel wall, and the drum was rotated through a long rod hinged to the rim of the drum. The pressure lengthened the vessel walls ($\sim 0.2-0.3 \text{ mm}$), thus turning the drum through an angle $\sim 2-3^\circ$ in proportion to the applied pressure. As a result, the change ΔS of the area of the extremal section of the Fermi surface was due both to pressure, $(\partial S / \partial p) \Delta p$, and to rotation of the sample, $(\partial S / \partial \theta) \Delta \theta$. At orientations such that $\partial S / \partial \theta$ for the given section is close to zero, our present results and the data of Ref. 13 are close, while for orientations where $\partial S / \partial \theta$ is large, the discrepancy between the results is also large.

Another source of error may be that in Ref. 13 no Fourier analysis was made of the recorded oscillations, and in particular no Fourier analysis was made of the individual shifts in the case of beats between close frequencies. This source of error, however, seems less significant than the rotation of the crystal.

The authors take the opportunity to thank A. I. Likhter for constant interest in the work, and R. G. Arkhipov, O. A. Voronov, and A. P. Kochkin for a discussion of the results.

¹W. A. Harrison, Phys. Rev. 118, 1190 (1960); 126, 497 (1962).

²R. W. Stark and L. M. Falicov, Phys. Rev. Lett. 19, 759 (1967).

³A. S. Joseph and W. L. Gordon, Phys. Rev. 126, 489 (1962).

⁴R. J. Higgins, J. A. Markus, and D. W. Whitmore, Phys. Rev. 137, A112 (1965).

⁵V. A. Venttsel', A. I. Likhter, and A. V. Rudnev, Pis'ma Zh. Eksp. Teor. Fiz. 4, 216 (1966) [JETP Lett. 4, 148 (1966)].

⁶V. A. Venttsel', A. I. Likhter, and A. V. Rudnev, Zh. Eksp. Teor. Fiz. 53, 108 (1967) [Sov. Phys. JETP 26, 73 (1968)].

⁷V. A. Venttsel', Zh. Eksp. Teor. Fiz. 55, 1191 (1968) [Sov. Phys. JETP 28, 622 (1969)].

⁸S. Rudin and R. W. Stark, The de Haas-van Alphen Spectrum of Zinc, Preprint, University of Chicago, Chicago, Illinois.

⁹R. Fletcher, L. Mackinnon, and W. D. Wallace, Philos. Mag. 20, 245 (1969).

¹⁰M. J. Lea, J. D. Llewellyn, D. R. Peck, and E. R. Dobbs,

Applicability of Landau's theory to phase transitions in the vicinity of a tetracritical point

D. G. Sannikov

Institute of Crystallography, Academy of Sciences, USSR

(Submitted 27 April 1978; after revision, 10 July 1978)

Zh. Eksp. Teor. Fiz. 75, 1714-1720 (November 1978)

The structure of the more and of the less symmetric phases between which a phase transition occurs are regarded as being distorted with respect to a still more symmetric phase, which is called the parent phase. The distortions of structure of the phases are described by means of a single irreducible representation of the symmetry group of the parent phase. It is shown that when these distortions are small, i.e., when the phase transitions are close to a multicritical point on the phase diagram, the constants of Landau's theory for the transitions under consideration have anomalous values, which show up both in the temperature variations of thermodynamic quantities and in the narrowness of the range of inapplicability of Landau's theory. Within the framework of the Landau theory, these phase transitions can be only transitions of second order. The treatment is carried through for the case of an arbitrary type of two-dimensional irreducible representation of the symmetry group of the parent phase.

PACS numbers: 05.70.Jk, 64.60.Kw

It is known that Landau's¹ phenomenological theory applies well to structural phase transitions (so far it has not been possible to detect with certainty, for any crystal, a range of inapplicability of this theory). Moreover, the material constants of crystals contain no small parameter that might enable us to demonstrate a physical reason for the narrowness of this region, as is the case, for example, for phase transitions into the superconducting state.² As will be shown below, it is possible to demonstrate such a reason for a quite broad class of structural phase transitions. It is known that the structures of many crystals are often only slightly distorted with respect to more symmetric structures: the so-called pseudocubic and pseudohexagonal crystals and others. Such a slight distortion can also serve as the small parameter that determines the good applicability of Landau's theory to the structural phase transitions under consideration. In other words, the set of constants that characterizes the region of inapplicability of Landau's theory is a small quantity in proportion to the smallness of the distortion; and the other constants, determining the temperature variations of thermodynamic quantities, are anomalous.

Phase transitions from a more symmetric phase to a less symmetric will be treated below within the framework of Landau's theory; not, however, on the basis of a thermodynamic potential written for the more symmetric phase, but on the basis of the thermodynamic potential of a still more symmetric phase—the "parent phase,"³ with respect to whose structure the more and the less symmetric phases are only slightly distorted.

For definiteness, we shall consider phase transitions between phases that correspond to a single two-dimensional irreducible representation of the parent phase.

All possible two-dimensional (mathematically) irreducible representations of the space groups of crystal symmetry can be classified according to the degree of one of the two independent invariants. Designating the basis functions of the representation by η and ξ and introducing suitable polar coordinates ρ and φ ,

$$\eta = \rho \cos \varphi, \quad \xi = \rho \sin \varphi, \quad (1)$$

we can express the independent invariants I and I' in the form⁴

$$I = \rho^2, \quad I' = \rho^n \cos n\varphi, \quad (2)$$

where n is an integer; $n \geq 3$. Thus the two-dimensional irreducible representation, designated hereafter by E_n , can be characterized by the number n .

The thermodynamic potential Φ for the representation E_n can be written as a series of powers of the invariants I and I' of (2):

$$\Phi = \alpha I + \beta I^2 + \gamma I^3 + \dots + \alpha' I' + \beta' I'^2 + \dots + \beta'' I I' + \dots \quad (3)$$

To this potential, as follows from the condition that Φ shall be an extremum with respect to the variable φ ,

$$\partial \Phi / \partial \varphi = \Phi_{,\varphi} = \Phi_{,\varphi} I_{,\varphi} = (\alpha' + 2\beta' I' + \beta'' I) (-n\rho^n \sin n\varphi) = 0,$$

correspond four types of solution:

$$\begin{aligned} &0) \rho = 0, \\ &1), 2) \sin n\varphi = 0, \quad \cos n\varphi = \mp 1, \\ &3) \cos n\varphi = -\frac{\alpha' + \beta'' \rho^2}{2\beta' \rho^n}, \end{aligned} \quad (4)$$